HKIE Transactions, 2015
Vol. 22, No. 4, 223–234, http://dx.doi.org/10.1080/1023697X.2015.1102654

A unified shear stress limit for reinforced concrete beam design

Daniel T W Looi[a†], Ray K L Su[a*] and Eddie S S Lam[b]

[a]*Department of Civil Engineering, The University of Hong Kong, Pokfulam Road, Hong Kong, People's Republic of China;*
[b]*Department of Civil and Environmental Engineering, The Hong Kong Polytechnic University, Hung Hom, Kowloon, Hong Kong, People's Republic of China*

(*Received 13 January 2015; accepted 6 August 2015*)

Nine asymmetrically spanned reinforced concrete deep beams were designed and tested to unreinforced web crushing failure in this experimental study to establish the appropriate shear stress limit for beam design. The lower bound and mean shear design limits associated with the concrete strut crushing in the web of the beam are identified, based on the better correlated concrete compressive strength parameter rather than its square root. A unified shear stress limit model is proposed to anchor the maximum strut crushing limit and sectional shear stress in design codes via a generic shear enhancement factor. The proposed unified model exhibits modest conservatism compared to the Hong Kong Code of Practice for Structural Concrete 2013 and the Chinese Code for Design of Concrete Structures (GB 50010). Transfer beams, pile caps and corbels, which are typically accompanied by high shear demand, can be optimised in size to leverage construction material cost savings through the more relaxed shear stress limit proposed in this study, which is justified through experiments.

Keywords: shear enhancement factor; shear stress limit; high-strength concrete; deep beam; strut-and-tie method; transfer girder

Introduction

The shear resistance of reinforced concrete (RC) beams is commonly assumed to be provided by concrete (apart from stirrups) through (1) uncracked regions in the flexural compression zone, (2) aggregate interlocking mechanisms, (3) residual tensile stresses across diagonal shear cracks and (4) dowel action of the longitudinal tension reinforcement. Besides the aforementioned beam actions, the arch action (via a direct compression strut) by the measure of shear span-to-depth (a/d) ratio is known to have substantial influence on the shear capacity of concrete. Hence, shear designs using a sectional shear stress limit check in typical slender beams and magnify with a shear enhancement factor in deep beams are common practices. The strut-and-tie model (STM), however, is commonly used in disturbed regions (D-regions, e.g. deep beams, pile caps, corbels, coupling beams and squat walls) having an enhanced shear limit due to direct strut action. These two approaches appear to be independent from each other and to date, there has been little discussion about unifying them.

Most design standards recommend a shear design limit to prevent strut crushing failure, but rather than associating this limit with the strut capacity in the STM, they are primarily benchmarked on past experimental data. It was discovered that even with an up-to-date database of past experiments to establish shear design principles in deep beams, data relating to high-strength concrete is exceptionally scarce.[1,2] Considering that the shear limit stipulated in the design codes (e.g. BS 8110 [3] and the Hong Kong Code of Practice for Structural Use of Concrete 2013, hereafter referred to as BD 2013 [4]) is mainly based on the results of normal-strength concrete, there is a need to re-evaluate the shear design limit for high-strength concrete, particularly in D-regions in the range of $a/d \leq 2$.

This paper investigates the contribution of strut angles (or a/d) and concrete strength towards the unreinforced web in the D-region of a deep section via a systematically designed experimental programme. The results are reconciled with provisions in design codes and the literature, in order to formulate the web crushing shear stress limit and its shear enhancement relationship in the D-region. A unified ultimate shear stress limit model is proposed as a first-tier simplified shear limit check, prior to the more rigorous higher-tier STM method.

Concrete shear stress limit

BS 8110 method

The concrete design shear stress capacity and its limit in RC beams described in BS 8110 Cl. 3.4.5.2 [3] can be

*Corresponding author. Email: klsu@hku.hk
†The author was 35 years old or younger at the time of his/her paper submission.

computed as follows:

$$v_c = 0.79(\rho)^{1/3}\left(\frac{400}{d}\right)^{1/4}\left(\frac{f_{\mathrm{cu}}}{25}\right)^{1/3}/\gamma_{\mathrm{shear}} \leq \text{ lesser of } [0.8\sqrt{f_{\mathrm{cu}}}, 5\,\mathrm{MPa}]. \quad (1)$$

This empirical equation has the functions of longitudinal bar dowel action (maximum 3% ρ), a depth factor ($400/d \geq 1$) and a maximum cube strength of 40 MPa. The limit to prevent strut crushing failure by taking the lesser of $0.8\sqrt{f_{\mathrm{cu}}}$ or 5 MPa has accounted for the 1.25 material partial safety factor. BS 8110 recognises the enhanced shear strength of sections close to supports and hence recommends the factor of $2d/a$ to increase shear stress, computed via Equation (1). It is however ironic that the shear limit remains the same, despite the provision of shear enhancement.

BD 2013 method

The BD 2013 [4] code was formulated with heavy referencing of BS 8110 [3], albeit with subtle alterations to suit the conditions specific to Hong Kong. Equation (2) shows the empirical shear model and its revised limit in BD 2013 Cl. 6.1.2.5. [4] as follows:

$$v_c = 0.79(\rho)^{1/3}(400/d)^{1/4}\left(\frac{f_{\mathrm{cu}}}{25}\right)^{1/3}/\gamma_{\mathrm{shear}} \leq \text{lesser of } [0.8\sqrt{f_{\mathrm{cu}}}, 7\,\mathrm{MPa}]. \quad (2)$$

Adjustment was made to allow for the common use of higher strength concrete in Hong Kong (maximum of 80 MPa cube strength in shear design), and the depth factor for members without stirrups should not be taken as less than 0.67 (as opposed to the minimum of 1 in BS 8110 [3]). The same shear enhancement factor of $2d/a$ is recommended but the 7 MPa shear limit remains unchanged.

GB 50010 [5] method

The mainland Chinese code GB 50010 [5] stipulates a clear distinction between slender beams (Cl. 6.3.3), D-regions in slender beams (Cl. 6.3.4) and deep beams (Appendix G). The shear provisions in these beams can be estimated using Equations (3a) to (3c), with the common shear limits shown in Equations (3d) and (3e). Cube strength nomenclature f_{cu} is adopted for uniformity in this paper.

For slender beams, they are estimated as follows:

$$v_c = 0.7(0.7 + 20\rho)\ (800/d)^{1/4}\frac{f_{tk}}{\gamma_{\mathrm{shear}}}. \quad (3a)$$

For D-regions in slender beams, they are estimated as follows:

$$v_c = \frac{1.75}{(a/d)+1}\frac{f_{tk}}{\gamma_{\mathrm{shear}}} \quad (\text{for } 1.5 \leq a/d \leq 3.0). \quad (3b)$$

For deep beams with point load, they are estimated as follows:

$$v_c = \frac{1.75}{(a/d)+1}\frac{f_{tk}}{\gamma_{\mathrm{shear}}} \begin{bmatrix} \text{if } a/d \leq 0.25, & \text{then } a/d = 0.25 \\ \text{if } 0.25 \leq a/d \leq 3.0, & \text{then } a/d \end{bmatrix}. \quad (3c)$$

Common shear limit for slender beams is estimated as follows:

$$\begin{aligned} v_c &\leq 0.25\beta_c f_{\mathrm{cu}} \quad \text{for } D/b \leq 4 \text{ (thick web)}, \\ v_c &\leq 0.20\beta_c f_{\mathrm{cu}} \quad \text{for } D/b \geq 6 \text{ (thin web)}. \end{aligned} \quad (3d)$$

Common shear limit for deep beams is estimated as follows:

$$\begin{aligned} v_c &\leq \frac{1}{60}\left(10 + \frac{L'}{D}\right)\beta_c f_{\mathrm{cu}} \quad \text{for } D/b \leq 4 \text{ (thick web)}, \\ v_c &\leq \frac{1}{60}\left(7 + \frac{L'}{D}\right)\beta_c f_{\mathrm{cu}} \quad \text{for } D/b \geq 6 \text{ (thin web)}, \end{aligned} \quad (3e)$$

where $\beta_c = 1.0$ ($f_{\mathrm{cu}} < 50$ MPa) and 0.8 (50 MPa $\leq f_{\mathrm{cu}} \leq 80$ MPa).

The depth factor for slender beams considered in GB 50010 [5] is between depth (d) 800 mm and 2000 mm. In comparison to BS 8110 [3] and BD 2013 [4], higher strength concrete is catered for in the shear limit with the provision of thick and thin webs. The implied strut angle with respect to horizontal ties lies between 33° and 76°, calculated via the a/d ratio. In conjunction with the arch phenomenon, the shear enhancement factor is identified as $1.75/(a/d + 1)$. Interestingly, the concrete characteristic tensile strength (f_{tk}) is used as the parameter for estimating shear rather than the concrete cylinder strength (f_c') or the cube strength (f_{cu}). It is worth noting that the material partial safety factor recommended in GB 50010 [5] is 1.4. The subtle difference in the codes contributes to variations in shear strength limit.

Other models

Hong and Ha [6] proposed a mean physical model based on the diagonal cracking phenomenon between intersection points of strut and flexural tension zone by reducing the corresponding strut width after flexural crack for the effective capacity of a concrete strut. The model, which is suitable for the intermediate a/d ratio, is restated in Equations (4a) and (4b). The model predicts the mean value and a safety factor 0.8 is suggested for conservatism.

For slender beams, where $2.0 < a/d \leq 4.0$, they are estimated as follows:

$$v_c = \frac{3}{4} f_c{}' \frac{\zeta^2 (1-\zeta)\ (1+\zeta-\zeta^2)}{a/d} \times 0.8. \qquad (4a)$$

For deep beams, where $0 \leq a/d \leq 2.0$, they are estimated as follows:

$$v_c = \frac{3}{4} f_c{}' \left[1 - \frac{a/d(1-\zeta)}{2}\right] \frac{\zeta(1-\zeta)(1+\zeta-\zeta^2)}{a/d} \times 0.8, \qquad (4b)$$

where $\zeta = 1.53 \sqrt[3]{\rho}$.

In view of the fact that more shear tests were being carried out around the world, Kuo et al. [7] proposed a new empirical model incorporating the arch action factor and the flexural-compression zone factor. The shear limit 0.83 MPa implicitly indicates a maximum *a*/*d* ratio of 1.63 (approximately 31.5° strut angle):

$$v_c = 1.17(a/d)^{-0.7} \quad \leq 0.83 \text{ MPa}. \qquad (5)$$

Experimental programme

The inconsistencies of shear enhancement due to arch action and its shear limit observed from the aforementioned models triggered the need to reconcile the shear stress limit in the D-region with a suite of systematically designed experimental specimens. In this study, nine asymmetrically spanned (hereafter referred to as "shear span") RC deep beams were designed in accordance with STM principles in order to synchronise and establish the web crushing shear limit. Only the shorter shear span was designed without stirrups, to form a diagonal compression strut failure mode.

Design parameters

Two design parameters were varied systematically in this study: the primary strut angle with respect to horizontal tension tie and the concrete compressive strength. The strut angle was designed to the nearest of 30°, 45° and 60° (corresponding to a shear span-to-lever arm ratio [*a*/*z*] of approximately 1.73, 1.00 and 0.58, respectively). In view of the scarcity of experimental data in relation to high-strength concrete in the D-regions in conjunction with a steep strut angle (> 45°), the concrete cube strength (f_{cu}) was varied, ranging from 33.9 MPa to 97.0 MPa. Table 1 shows the test matrix, which classifies the nine specimens according to concrete strength and strut angle.

Design and detailing of test specimens

The deep beams were designed to use the STM following the guidelines outlined in Section A of ACI 318 [8], with

Table 1. Test matrix and details of specimens.

Type*	L (mm)	L' (mm)	a (mm)	anc. (mm)	$H_{stirrups}$	$V_{stirrups}$	Long. bars.	ρ (%)	h_{Long} (mm)	z (mm)	a/z	θ (°)	f_{cu} (MPa)
C30-1.7	2000	1600	600	100	R8@80	R10@110	6 T10	1.00	135	336.5	1.78	29.3	34.1
C60-1.7	2000	1600	600	100	R8@80	R10@70	4 T16	1.71	110	330.5	1.82	28.8	64.7
C90-1.7	2000	1600	600	100	R8@80	R10@55	6 T16	2.57	145	308.1	1.95	27.2	89.5
C30-1.0	1750	1300	300	150	R8@80	R10@80	6 T12	1.44	147	339.2	0.88	48.5	34.8
C60-1.0	1750	1300	300	150	R8@80	R10@55	6 T16	2.57	145	330.7	0.91	47.8	66.1
C90-1.0	1750	1300	300	150	R8@80	R10@40	4 T16 + 2 T20	3.05	146	317.1	0.95	46.6	97.0
C30-0.5	1585	1170	170	115	R8@80	R10@110	6 T12	1.44	147	341.5	0.50	63.5	33.9
C60-0.5	1585	1170	170	115	R8@80	R10@60	4 T16	1.71	110	336.7	0.50	63.2	65.3
C90-0.5	1585	1170	170	115	R8@80	R10@50	6 T16	2.57	145	353.8	0.48	64.3	92.6

Note: *The first three characters represent the target concrete compression strength and the one decimal place number after the hyphen denotes the *a*/*z* ratio; for example C30-1.7 represents a beam with a target 30 MPa concrete strength and a 1.7 *a*/*z* ratio.

the node, bearing and strut efficiency factors referred to in Su and Chandler [9]. The specimens were subjected to a single point load, with a pinned support at the shorter shear span and a roller support at the other end to allow horizontal movements, avoiding any unanticipated compression effect forming at the tension tie of the STM. The longer shear span was predetermined at 1 m and the shorter shear span was varied to form the diagonal strut angle. The dimensions of the beams were designed with three distinct lengths: the 30° strut angle beams were 2 m long, the 45° strut angle beams were 1.75 m long and the 60° strut angle beams were 1.585 m long. The width was fixed at 100 mm and the depth at 470 mm. The concrete cover was taken as 10 mm at the top and side and 30 mm at the bottom to make allowances for the embedded steel plates.

Two 300 × 100 × 20 mm steel plates were embedded at the soffit of each specimen to provide smooth surfaces to be seated on the supports. An external 200 × 150 × 20 mm top loading plate was provided at the loading point to offer a smooth surface when in contact with the actuator. Both the bottom plate at the shorter shear span and the top loading plate were predrilled with holes to tightly fit R8 bars, which formed a cage for node confinement and protection in order to prevent local premature crushing.[10,11] The dimension and reinforcement arrangement of the STM-designed test specimens are presented in Figure 1 and the details are displayed in Table 1.

Materials

All concrete used to cast the specimens was mixed and cast in situ in the concrete technology laboratory at The University of Hong Kong. The concrete had a maximum aggregate size of 10 mm and was mixed with ordinary Portland cement, sand (as fine aggregate) and water, in addition to superplasticisers to improve workability owing to the congested reinforcement configuration, especially in the 45° strut angle beams. Eight

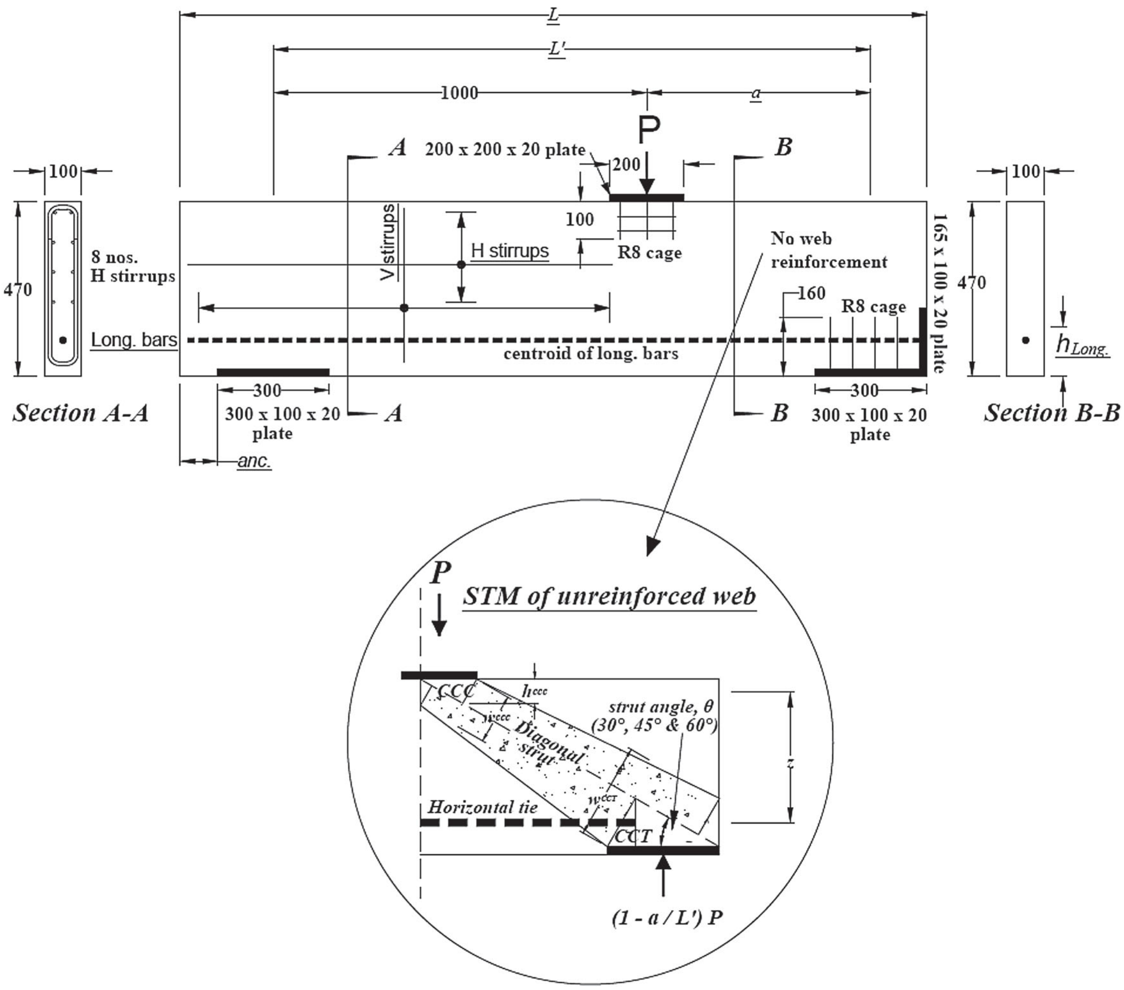

Figure 1. Specimen details and STM idealisation.

Table 2. Properties of steel reinforcement.

Type of steel reinforcement	A_s (mm^2)	E (GPa)	f_y (MPa)	f_u (MPa)
R8	48.3	207	289	514
R10	74.6	208	289	358
T12	109.6	224	602	701
T16	195.0	193	592	706
T20	308.1	186	578	665

150 × 150 × 150 mm cubes and two standard cylinders of 150 mm diameter and 300 mm height were also cast during the pouring of the concrete to serve as controls of concrete strength evaluation. All concrete was covered with plastic sheets and left for curing.

All longitudinal reinforcement was made of $f_y = 500$ Mpa, with T12, T16 and T20 deformed bars, while all stirrups and cages were made of $f_y = 250$ Mpa, with R8 and R10 round bars. The reinforcement was ordered from a single local steel supplier. The measured concrete cube strengths are given in Table 1 and the steel properties are shown in Table 2.

Set-up, instrumentation and testing procedure

The specimens were supported on roller support at the longer shear span and pinned support at the shorter shear span. Two test rigs were used for the beam tests. All beams (except C90-1.0 and C90-0.5) were tested in a 1000 kN loading frame using servo-controlled actuator with a 1000 kN capacity. Due to the higher loading demand, the C90-1.0 and C90-0.5 beams were tested using a servo-controlled actuator with a 10,000 kN capacity in a self-reaction hydraulic frame. Both actuators were connected to an MTS system and the loading arrangements are shown in Figure 2, with single point loading acting vertically on the centre of the loading plate in addition to the self-weight of the beams. High-strength grout was used as packing material to fill the gap in between the loading plate and the actuator. Proper safety measurement was given to prevent concrete blocks from falling after brittle failure of the unreinforced web panel.

Point deformation was measured with linear voltage displacement transducers (LVDTs), with the layout shown in Figure 2. Four LVDTs were put in a row spaced horizontally at 250 mm and were situated 130 mm below the top of the beam to monitor the vertical displacement. Two LVDTs were put directly at the top of the beam (vertically aligned with the supports) in order to detect early support vertical settlement for error correction. Four additional horizontal LVDTs were put at the side faces of the beam to monitor longitudinal and rotational deformations. During testing, a monotonic point load was applied at the loading plate on top of the beam with an increment rate of 0.005 mm/s until strut failure (approximately 20% drop after peak load).

Observed response

Initial flexural tensile microcracks at the soffit of the beam propagated vertically to the topmost longitudinal bars at a fairly slow rate and remained as fine

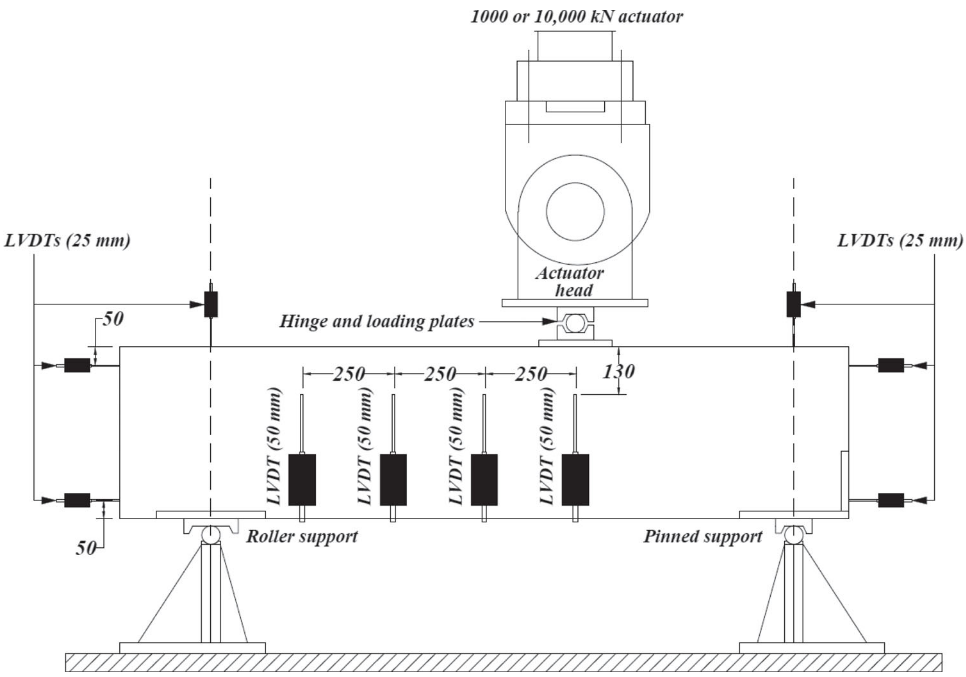

Figure 2. Testing set-up and instrumentation.

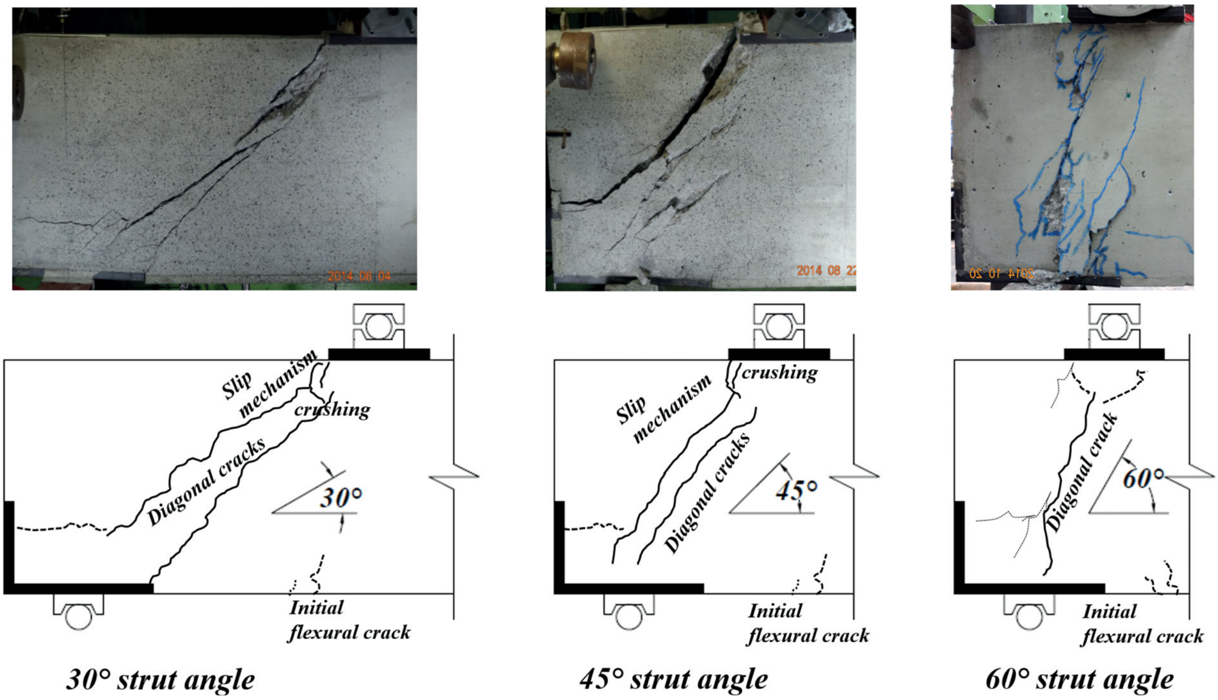

Figure 3. Typical crack pattern of specimens.

cracks. At about 25% of the peak shear load, diagonal cracks formed at the centre of the unreinforced web. Despite the appearance of diagonal cracks, the specimens still exhibited much reserved strength before reaching their ultimate peak load. Slip mechanism was observed at the vicinity of peak load, crushing the adjacent concrete at the outer edge of top loading plate. The concrete failed in a brittle manner and often accompanied by loud noise, but collapse was prevented due to the presence of longitudinal reinforcement, the protection cage and the transverse stirrups at the longer shear span. Figure 3 shows typical crack patterns of the unreinforced web panel after failure.

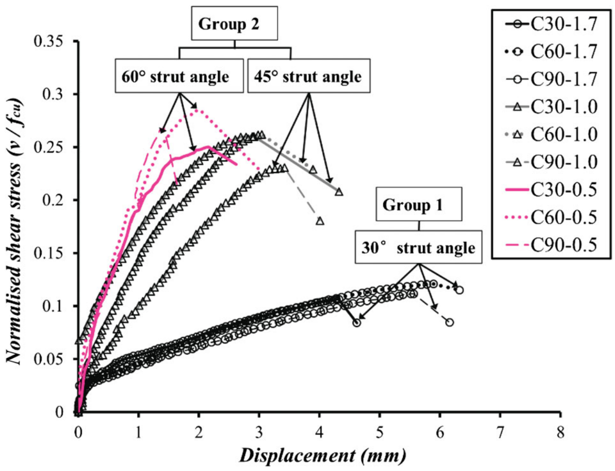

Figure 4. Normalised shear stress versus vertical displacement.

Analysis of test results and discussion

Normalised shear stress versus deflection curves, peak shear stress and strut efficiency factor

Figure 4 shows the normalised shear stress versus deflection curves with respect to different target concrete compressive cube strengths, to account for asymmetrical shear span and variation of concrete strength. Early support displacement was subtracted to obtain the absolute displacements of the specimens. The shear stress (V/bd_{shear}) is calculated with the assumption of $d_{\text{shear}} = 0.8D$. Based on the cluster of the results, two groups were identified; Group 1 ($a/z = 1.7$) shows generally lower peak stress in contrast to Group 2 ($a/z \leq 1.0$). A simplification was made to Figure 4, limiting it to a 20% drop after the peak load.

Table 3 shows the peak load obtained from the experiment. Computation was carried out to obtain the peak shear stress and strut efficiency factor. It is not possible to claim any representative shear stress limit based on the limited nine specimens, hence, further data was collected to corroborate the results.

Corroboration with deep beams without stirrups shear data collected from the literature

Strict filter criteria were imposed in controlling the validity of data taken from a large pool of literature published

Table 3. Experimental peak loads, shear stresses and strut efficiency factors.

Type*	P (kN)	V (kN)	v_c (MPa)	v_c/f_{cu}	w_{CCC} (mm)	$f_{strut\ CCC}$ (MPa)	β
C30-1.7	218.4	136.5	3.63	0.11	129.9	21.5	0.63
C60-1.7	471.6	294.8	7.84	0.12	133.0	46.0	0.71
C90-1.7	602.7	376.7	10.02	0.11	151.5	54.4	0.61
C30-1.0	443.8	341.4	9.08	0.26	165.8	27.5	0.79
C60-1.0	847.6	652.0	17.34	0.26	169.7	51.9	0.79
C90-1.0	1110.0	853.9	22.71	0.23	178.8	65.7	0.68
C30-0.5	376.4	321.7	8.55	0.25	177.6	20.2	0.60
C60-0.5	819.5	700.4	18.63	0.29	179.0	43.8	0.67
C90-0.5	1107.5	946.6	25.18	0.27	181.3	58.0	0.63

Note: *The first three characters represent the target concrete compression strength and the one decimal place number after the hyphen denotes the a/z ratio; for example C30-1.7 represents a beam with a target 30 MPa concrete strength and a 1.7 a/z ratio.

Table 4. Filtered database of deep beams without stirrups.

Reference	No. of specimens	Beam label	f_{cu}* (MPa)	d (mm)	a/d	θ (°)	β	v_c/f_{cu}
Quintero-Febres et al. [12]	6	A3, A4, B3, B4, HA3, HB3	27.1 to 60.4	460	0.8 to 1.4	34.9 to 50.9	0.96 to 1.18	0.13 to 0.21
Moody et al. [13]	7	24a, 24b, 25b, 27a, 27b, 28a, 28b	21.2 to 28.7	609.6	1.5	33.3	1.07 to 1.27	0.12 to 0.16
Smith and Vantsiotis [14]	4	0A0-44, 0A0-48, 0C0-50, 0D047	24.4 to 26.1	349	1.0 to 2.0	26.4 to 45.0	1.07 to 1.20	0.11 to 0.19
Yang et al. [15]	2	L5-40, L5-60	38.7	400 to 600	0.5 to 1.1	41.5 to 61.6	1.25 to 1.30	0.18 to 0.23
Sahoo et al. [16]	2	BN-0-0, BN-0-0 (R)	48.8 to 55.2	450	0.5	62.1	0.86 to 0.91	0.19 to 0.20
Total	**21**	–	**21.2 to 60.4**	**349 to 609.6**	**0.5 to 2.0**	**26.4 to 62.1**	**0.86 to 1.27**	**0.11 to 0.23**

Note: *f_{cu} is assumed to be 37/30 f_c'.

between 1954 and 2009. The criteria include: (i) strut failure only (bending, bearing and node failure are ruled out); (ii) sufficient data to compute the strut efficiency factor without assumption (e.g. missing data of loading plate width); and (iii) elimination of suspicious data (e.g. an efficiency factor which is much higher than unity measured in cube strength and specimens failing in the lower peak shear despite having a higher concrete strength). Finally, a set of high-quality data from 21 deep beams without stirrups was successfully collected from the literature to complement the results of the nine specimens in this study (see the summary in Table 4).[11–15] The data span across values of f_{cu} ranging from 21.2 MPa to 60.4 MPa and strut angles of 26.4° to 62.1°. Non-hydrostatic nodes were used to calculate the strut width and the a/d ratio was used to ensure conformation to the information given in the literature.

Strut efficiency factor recommendation

The full efficiency of unreinforced strut strength can be compounded into a single strut efficiency factor (β) to account for stress disturbance, concrete uniaxial strength, strut angle, orientation, narrower strut width and the extent of cracks and degree of lateral confinement as follows:

$$\beta = \frac{f_{strut}}{f_{cu}} = \frac{(1 - a/L')\,P}{\sin(\theta)\; b\; w f_{cu}}. \tag{6}$$

The computed strut efficiency factors are shown in Table 3. In view of the consistently high efficiency factor (an average of 0.68) achieved in this study and referenced from the collected database, it is provisionally justified to adopt a constant nominal strut factor of 0.6. A factor of 0.85 (similar to the recommendation in ACI 318 [8] and approximately equal to the reciprocal of the shear factor 1.25 in BD 2013 [4]) is introduced to account for the strut stress-strain field and truss model uncertainties. Hence, compounding the 0.85 uncertainty factor with the nominal strut factor 0.6, the effective strut efficiency factor is 0.5, which is lower than the maximum 0.67 factor commonly used for rectangular stress blocks in a compression zone.

Table 5. Statistical analysis for shear stress with respect to concrete strength and the square root of concrete strength.

Group 2 specimens	Beam label	Beam reference	v_c/f_{cu}	$v_c/\sqrt{f_{cu}}$
45° (database)	0A0-44	[14]	0.19	0.97
	0A0-48	[14]	0.18	0.94
	B3	[12]	0.21	1.34
	B4	[12]	0.21	1.32
	HB3	[12]	0.21	1.61
45° (this study)	C30-1.0	This study	0.26	1.54
	C60-1.0	This study	0.26	2.13
	C90-1.0	This study	0.23	2.31
60° (database)	L5-40	[15]	0.23	1.40
	L5-60	[15]	0.18	1.12
	BN-0-0	[16]	0.20	1.38
	BN-0-0 (R)	[16]	0.19	1.41
60° (this study)	C30-0.5	This study	0.25	1.47
	C60-0.5	This study	0.29	2.31
	C90-0.5	This study	0.27	2.62
mean	–	–	**0.22**	**1.59**
standard deviation	–	–	**0.0338**	**0.4952**
standard deviation/ mean	–	–	**0.153**	**0.311**

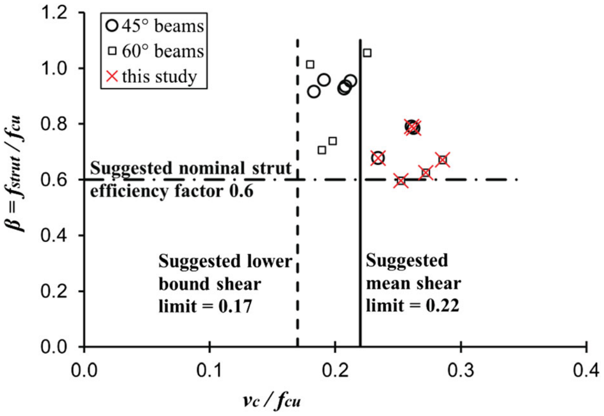

Figure 5. Relationship of the strut efficiency factor and normalised shear stress of the Group 2 beams.
Note: Partial safety factor is excluded for shear limit.

Shear enhancement factor and the unified shear stress limit model

The conventional shear stress limit for sectional design has a function of the square root of concrete strength ($\sqrt{f_{cu}}$) as a measure of concrete tensile strength (ACI 318 commentary R11.2.2.1 [8]). However, if a cap limit is imposed and is primarily intended for strut crushing failure prevention (not diagonal tensile failure), using the square root of concrete strength as the dependent parameter is questionable. A statistical analysis of shear stress was carried out for the Group 2 specimens (Table 5). The results were evident that shear stress has stronger correlation with concrete strength (almost double) rather than its square root. Figure 5 shows the relationship between

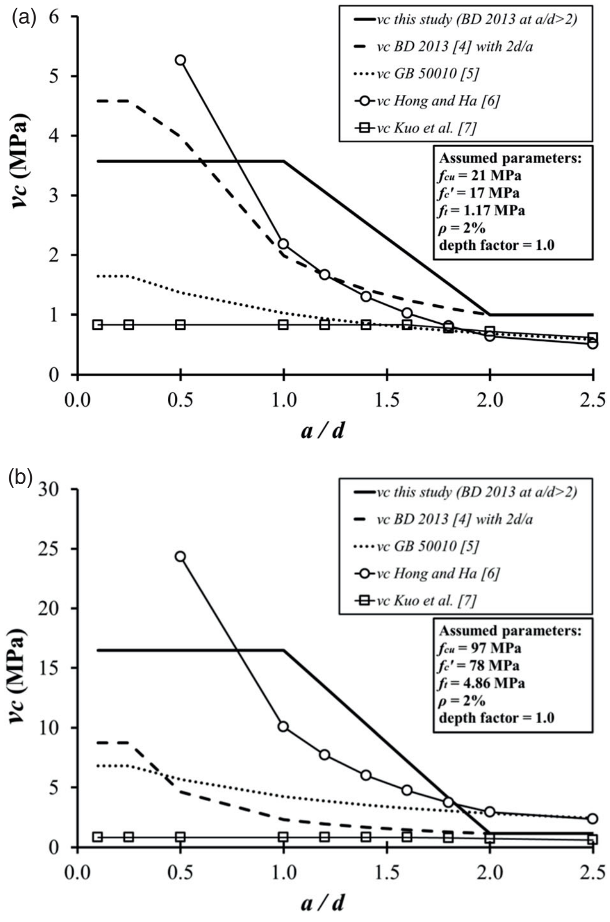

Figure 6. (a) Variation of shear strength models for low-strength concrete; (b) variation of shear strength models for high-strength concrete.
Note: Partial safety factor is excluded for shear limit.

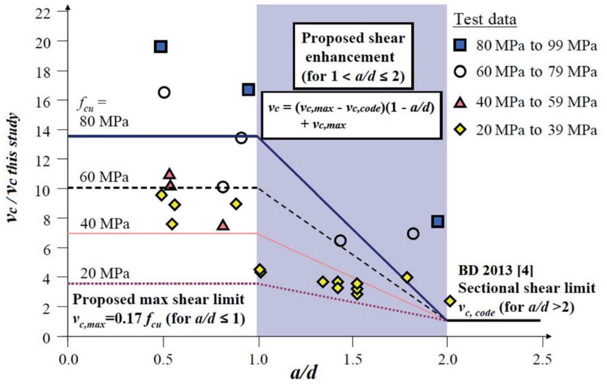

Figure 7. Unified shear stress limit model (for low- and high--strength concrete), with BD 2013 [4] as an example.
Note: Partial safety factor is excluded for shear limit.

the suggested nominal concrete strut efficiency factor and normalised shear stress. Only Group 2 beams are considered owing to the consistent shear stress obtained in this test. A suggested lower bound shear limit corresponding

Table 6. Comparison of experimental and database results with various models.

			This study		BD 2013 [4]		GB 50010 [5]		Hong and Ha [6]		Kuo et al. [7]	
Beam label	Beam reference	v_c (MPa)	$v_{c\ \mathrm{proposed}}$ (MPa)	$v_c/v_{c\ \mathrm{proposed}}$	$v_{c\ \mathrm{BD}\ 2013}$ (MPa)	$v_c/v_{c\ \mathrm{BD}\ 2013}$	$v_{c\mathrm{GB}\ 50010}$ (MPa)	$v_c/v_{c\ \mathrm{GB}\ 50010}$	$v_{c\ \mathrm{HH}}$ (MPa)	$v_c/v_{c\ \mathrm{HH}}$	$v_{c\ \mathrm{K}}$ (MPa)	$v_c/v_{c\ K}$
30° strut angle												
24a	[13]	3.41	2.57	1.33	1.45	2.35	1.55	2.21	2.01	1.70	0.83	4.11
24b	[13]	3.49	2.83	1.23	1.46	2.39	1.60	2.17	2.29	1.52	0.83	4.20
25b	[13]	3.33	2.51	1.33	1.50	2.22	1.47	2.26	2.02	1.65	0.83	4.02
27a	[13]	4.00	2.92	1.37	1.48	2.71	1.67	2.40	2.38	1.68	0.83	4.82
27b	[13]	4.10	3.09	1.33	1.51	2.71	1.66	2.47	2.55	1.61	0.83	4.94
28a	[13]	3.49	3.16	1.10	1.57	2.22	1.69	2.06	2.74	1.27	0.83	4.20
28b	[13]	3.92	3.06	1.28	1.55	2.53	1.63	2.41	2.64	1.49	0.83	4.72
0C0-50	[14]	4.06	3.46	1.17	1.63	2.49	1.76	2.31	2.64	1.54	0.83	4.89
0D0-47	[14]	2.58	1.07	2.40	1.07	2.40	1.29	2.00	1.12	2.31	0.72	3.59
A3	[12]	4.00	3.32	1.21	1.52	2.63	1.66	2.41	2.60	1.54	0.83	4.82
A4	[12]	3.55	3.32	1.07	1.52	2.34	1.66	2.13	2.60	1.37	0.83	4.28
HA3	[12]	7.93	6.55	1.21	1.71	4.64	2.71	2.93	5.68	1.40	0.83	9.56
C30-1.7	This study	3.63	2.04	1.78	1.00	3.64	1.65	2.20	1.56	2.33	0.78	4.65
C60-1.7	This study	7.84	3.00	2.61	1.23	6.35	2.51	3.12	3.55	2.21	0.77	10.19
C90-1.7	This study	10.02	2.07	4.83	1.32	7.58	3.32	3.01	4.97	2.02	0.73	13.64
Sub mean	–	–	–	1.68	–	3.28	–	2.41	–	1.71	–	5.78
SD	–	–	–	0.95	–	1.59	–	0.33	–	0.33	–	2.82
45° strut angle												
0A0-44	[14]	4.90	4.33	1.13	2.15	2.28	2.03	2.42	4.02	1.22	0.83	5.90
0A0-48	[14]	4.78	4.42	1.08	2.17	2.21	2.07	2.31	4.10	1.17	0.83	5.76
B3	[12]	8.48	6.79	1.25	2.73	3.10	2.72	3.12	8.14	1.04	0.83	10.21
B4	[12]	8.32	6.79	1.22	2.73	3.04	2.72	3.06	8.14	1.02	0.83	10.02
HB3	[12]	12.50	10.26	1.22	3.01	4.16	3.64	3.44	12.98	*0.96*	0.83	15.06
C30-1.0	This study	9.08	5.92	1.53	2.29	3.97	2.49	3.65	6.14	1.48	0.83	10.94
C60-1.0	This study	17.34	11.23	1.54	2.84	6.12	3.79	4.58	12.68	1.37	0.83	20.89
C90-1.0	This study	22.71	16.49	1.38	2.86	7.93	5.45	4.16	18.07	1.26	0.83	27.36
Sub mean	–	–	–	1.29	–	4.10	–	3.34	–	1.19	–	13.27
SD	–	–	–	0.16	–	1.86	–	0.74	–	0.17	–	7.03
60° strut angle												
L5-40	[15]	8.73	6.58	1.33	3.45	2.53	3.06	2.85	11.37	*0.77*	0.83	10.52
L5-60	[15]	6.97	6.58	1.06	3.36	2.07	3.10	2.25	11.83	*0.59*	0.83	8.39
BN-0-0	[16]	9.66	8.30	1.16	3.58	2.70	3.60	2.68	15.33	*0.63*	0.83	11.63
BN-0-0 (R)	[16]	10.45	9.39	1.11	3.58	2.92	3.95	2.65	17.35	*0.60*	0.83	12.59
C30-0.5	This study	8.55	5.76	1.48	3.56	2.40	3.05	2.81	11.46	*0.75*	0.83	10.31
C60-0.5	This study	18.63	11.10	1.68	4.44	4.19	4.75	3.93	24.29	*0.77*	0.83	22.44
C90-0.5	This study	25.18	15.73	1.60	5.34	4.71	6.83	3.68	38.68	*0.65*	0.83	30.33
Sub mean	–	–	–	1.35	–	3.07	–	2.98	–	*0.68*	–	15.17
SD	–	–	–	0.23	–	0.91	–	0.56	–	0.07	–	7.49
Total mean	–	–	–	1.50	–	3.45	–	2.79	–	1.33	–	9.97
Total SD	–	–	–	0.71	–	1.59	–	0.66	–	0.49	–	6.95

Note: Shear stress check ratios below unity are italicised. The safety factor γ_{shear} 1.25 is excluded.

to the strut efficiency limit is identified as $0.17\,f_{cu}$ with a mean shear limit of $0.22\,f_{cu}$.

A generic shear enhancement factor (Equation (7b)) is thus put forward in the range of $1 < a/d \leq 2$, anchoring the aforementioned shear limit $0.17\,f_{cu}$ (lower bound) or $0.22\,f_{cu}$ (mean) (Equation (7a)) at the upper stream ($a/d \leq 1$) and at the lower stream ($a/d > 2$) using the sectional shear limit in various design codes (Equation (7c)):

$$\text{For } a/d \leq 1, \quad v_{c\ \text{proposed}} = v_{c\ \text{strut}} = 0.17\frac{f_{cu}}{\gamma_{\text{shear}}}\ \text{(lower bound)}; \quad \text{or } 0.22\frac{f_{cu}}{\gamma_{\text{shear}}}\ \text{(mean)}; \tag{7a}$$

$$\text{For } 1 < a/d \leq 2, \quad v_{c\ \text{proposed}} = (v_{c\ \text{strut}} - v_{c\ \text{code}})(1 - a/d) + v_{c\ \text{strut}}; \tag{7b}$$

$$\text{For } a/d > 2, \qquad v_c = v_{c\ \text{code}}. \tag{7c}$$

Comparison of the proposed unified shear stress limit model with design codes and the literature

The proposed unified lower bound shear stress limit model, which features a seamless transition at the $1 < a/d < 2$ interval and is anchored using BD 2013 [4] shear stress provision at the lower stream ($a/d > 2$), is compared to design codes BD 2013 [4] (with its original shear enhancement $2d/a$) and GB 50010 [5]. In addition to design codes, other researchers' models (i.e. Hong and Ha [6] and Kuo et al. [7]) are superimposed on Figure 6(a) for low concrete strength (21 MPa) and Figure 6(b) for high concrete strength (97 MPa), consistent with the range of concrete strength in the database collected. A typical longitudinal steel reinforcement ratio of 2% is used as an example and the depth factor is taken as unity. It can be seen from the variation of the plot in Figures 6(a) and 6(b) that different rates of shear enhancement in lower strength concrete and higher strength concrete are exhibited in relation to each of the design codes (i.e. BD 2013 [4] and GB 50010 [5]). The shear cap limit stipulated by the codes to prevent strut crushing entails a/d beyond a practical limit. This is evident of the flat plateau at $a/d > 0.25$ (approximately 76° strut angle). The model of Kuo et al. [7] is solely dependent on a/d and remains constant regardless of concrete strength, which results in an extreme lower bound model. Contrary to this, the model of Hong and Ha [6] has an obvious shear enhancement but no stated upper bound limit, which results in significant shear strength for $a/d \leq 1$.

A shear limit corresponding to the range of 20 MPa to 80 MPa is plotted in Figure 7 to further validate the proposed unified shear limit model. Although the lower bound shear limit of $0.17\,f_{cu}$ was proposed on the basis of Group 2 ($> 45°$ strut angle) results, it was found that Group 1 beams with a 30° strut angle are far above the enhanced shear limit in the transition zone of $1 < a/d \leq 2$. The upper stream ($a/d \leq 1$) using the lower bound shear limit compatible with the proposed strut efficiency factor and the lower stream ($a/d > 2$) by means of the sectional shear limit in the codes are expected to perform adequately above the safety margin. In this study, three high-strength concrete specimens ($f_{cu} > 89.5$ MPa) with different strut angles are plotted in the range of 80 MPa to 99 MPa to ensure the proposed shear limit is suitable for high-strength concrete. Hence, the proposed shear limit model is deemed to satisfy a wide range of concrete strengths and strut angles via the generic shear enhancement factor.

Table 6 shows the computed average shear stress results normalised with various models (with $\gamma_{\text{shear}} = 1$) for all beams tested in this study and collected from the literature. The proposed unified model and Hong and Ha's [6] model demonstrate excellent correlation, with 50% and 33% conservatism, respectively, in contrast to the extreme reservation by the lower bound empirical models stipulated in design codes. Although Hong and Ha's [6] model appears suitable for the intermediate range of a/d, it may underestimate some 45° strut specimens and all of the 60° beams, even after consideration of the 0.8 safety factor. Those specimens demonstrating shear stress check ratios below unity are italicised in Table 6.

Summary and conclusion

Nine asymmetrically spanned deep beams (shorter span without stirrups) were designed in accordance with STM principles and tested strictly to strut failure, ensured by node protection and various detailing. In addition, high-quality data from research encompassing a total of 21 deep beams without stirrups (which passed the strict filter criteria) were collected from the literature to complement this study.

It was discovered that shear stress due to the arch action in $a/d \leq 1$ correlates better with f_{cu} than with its square root. Hence, Group 2 beams ($> 45°$ strut angles) were used to calibrate the maximum shear stress limit to be consistent with the strut capacity. Two limits associated with strut failure were identified, $0.17\,f_{cu}$ (lower bound) and $0.22\,f_{cu}$ (mean). This paper puts forward a generic shear enhancement factor at the transition zone ($1 < a/d \leq 2$) in order to offer a seamless mechanism with which to anchor the upper stream strut limit ($1 \leq a/d$) and lower stream ($a/d > 2$) using sectional shear stresses stipulated in various design codes. Group 1 beams were found to be far above the enhanced shear limit at the transition zone. The proposed unified shear stress limit model was compared to BD 2013 [4], GB 50010 [5] and two other researchers' models [6,7] using the experimental results and the database. The unified model appears to be the modest, avoids over-conservatism and is sufficiently adequate for design purposes.

Through a more relaxed shear limit (i.e. the unified shear stress model), it is foreseen that the proposed model could be expanded into concrete web crushing shear limit checking for more D-regions in high-rise buildings (e.g. deep beams, pile caps, corbels, coupling beams and squat walls), in considering typical load cases and also a 2500-year return period seismic load for low-to-moderate earthquake regions such as Hong Kong. The unified shear stress limit model is proposed as a first-tier simplified shear limit check, prior to the more rigorous higher-tier STM method.

Funding

This work was supported by the Basic Research Funding of The University of Hong Kong [grant number 104003451].

Notes on contributors

Mr Daniel T W Looi obtained his B.Sc. Eng. (Hons) degree from University of Malaya, Kuala Lumpur, Malaysia. He is currently a Postgraduate Candidate under the supervision of Associate Professor, Ir Dr Ray Su in the Department of Civil Engineering at The University of Hong Kong. He worked as a Structural Engineer in both the high-rise building and plant industry for five years. He is a member of the Malaysia EC8 earthquake code annex drafting committee. His research interests include shear strength and the seismic design of concrete buildings in low-to-moderate seismicity regions.

Ir Dr Ray K L Su is an Associate Professor of Structural Engineering, the Department of Civil Engineering at The University of Hong Kong. He obtained his B.Sc. (Eng) and Ph.D. degrees from the University of Hong Kong. His current research interests lie in the development of new theories suitable for the seismic assessment and design of concrete and masonry structures, strengthening concrete members using external steel plates and the evaluation of the fracture properties of concrete and graphite. He is currently serving as the Secretary of Structural Discipline in the Hong Kong Institution of Engineers (HKIE) and acts as the Principal Investigator for some consultancy and research projects related to strengthening of concrete structures and seismic design of buildings.

Ir Dr Eddie S S Lam is an Associate Professor of Structural Engineering, the Department of Civil and Environmental Engineering at The Hong Kong Polytechnic University and has had a varied career in civil, structural and mechanical engineering. He received his Ph.D. degree in 1989 from the University of Southampton, the UK. His current interest is in the strengthening of concrete structures. He is a former Chairman of the HKIE Structural Division, a member of the HKIE Structural Discipline and a Council Member of the Institution of Structural Engineers (IStructE).

Notations

a	=	shear span between centreline of the load and support
b	=	beam width
d	=	beam effective depth
d_{shear}	=	beam depth for shear calculation, assumed as $0.8D$
f_c'	=	compressive cylinder strength of concrete
f_{cu}	=	compressive cube strength of concrete
$f_{\text{struct CCC}}$	=	strut stress adjacent to CCC node in the STM
f_{tk}	=	characteristic tensile strength of concrete
f_y	=	yield strength of steel reinforcement
f_u	=	tensile strength of steel reinforcement
h_{Long}	=	longitudinal bar height from soffit to centre of top layer bar
v_c	=	shear stress capacity of concrete
$v_{c\ \text{strut}}$	=	proposed shear stress capacity of concrete corresponding to the STM strut
$v_{c\ \text{code}}$	=	codified shear stress capacity of concrete
w	=	narrower strut width, in this case taken as the width adjacent to the CCC node
z	=	bending moment lever arm
A_s	=	steel reinforcement cross-section area
A_{eff}	=	effective shear cross-section area of concrete
D	=	beam total depth
E	=	Young's modulus
H_{stirrups}	=	horizontal stirrups
L	=	beam length
L'	=	clear span
P	=	applied point load
V	=	shear force
V_{stirrups}	=	vertical stirrups
β	=	strut efficiency factor
γ_{shear}	=	material partial safety factor for shear load
ρ	=	longitudinal reinforcement ratio
θ	=	strut angle with respect to horizontal tie

References

[1] Reineck KH, Todisco L. Database of shear tests for non-slender reinforced concrete beams without stirrups. ACI Struct J. 2014;111(6):1–10.

[2] Tuchscherer RG, Birrcher DB, Williams CS, Deschenes DJ, Bayrak O. Evaluation of existing strut-and-tie methods and recommended improvements. ACI Struct J. 2014;111(1):1–10.

[3] British Standards Institution (BSI). BS 8110-1: structural use of concrete – part 1: code of practice for design and construction. London, the UK: BSI; 1997.

[4] Hong Kong Buildings Department (BD). Code of practice for structural use of concrete 2013. HK: BD; 2013.

[5] National Standard of the People's Replublic of China. GB 50010: code for design of concrete structures. Ministry of Construction of the People's Republic of China, Beijing, China Architecture & Building Press; 2010.

[6] Hong SG, Ha T. Effective capacity of diagonal strut for shear strength of reinforced concrete beams without shear reinforcement. ACI Struct J. 2012;109(2): 139–148.

[7] Kuo WW, Hsu TTC, Hwang SJ. Shear strength of reinforced concrete beams. ACI Struct J. 2014;111(4):809–818.

[8] ACI Committee 318. Building code requirements for structural concrete (ACI 318–11) and commentary. Farmington Hills, MI: American Concrete institute; 2011.

[9] Su RKL, Chandler AM. Design criteria for unified strut and tie models. Progr Struct Eng Mater. 2001;3: 288–298.

[10] Zhang N, Tan KH. Size effect in RC deep beams: experimental investigation and STM verification. Eng Struct. 2007;29:3241–3254.

[11] Tan KH, Kong FK, Teng S, Weng LW. Effect of web reinforcement on high-strength concrete deep beams. ACI Struct J. 1997;94(5):572–581.

[12] Quintero-Febres CG, Parra-Montesinos G, Wight JK. Strength of struts in deep concrete members designed using strut-and-tie method. ACI Struct J. 2006;103(4): 577–586.

[13] Moody KG, Viest IM, Elstner RC, Hognestad E. Shear strength of reinforced beams. 1. tests of simple beams. ACI J. 1954;51(4):317–332.

[14] Smith KN, Vantsiotis AS. Shear strength of deep beams. ACI J. 1982;79(22):201–213.

[15] Yang KH, Chung HS, Lee ET, Eun HC. Shear characteristics of high-strength concrete deep beams without shear reinforcements. Eng Struct. 2003;25:1343–1352.

[16] Sahoo DK, Singh B, Bhargava P. An appraisal of the ACI strut efficiency factors. Mag Concrete Res. 2009;61(6):445–456.